



A ratiometric electrochemiluminescence sensing platform for robust ascorbic acid analysis based on a molecularly imprinted polymer modified bipolar electrode

Yue Hu^a, Yongcheng He^b, Zhengchun Peng^{c,*}, Yingchun Li^{a,c,**}

^a College of Science, Harbin Institute of Technology, Shenzhen, Guangdong, 518055, PR China

^b Department of Nephrology, Shenzhen Hengsheng Hospital, Shenzhen, Guangdong, 518102, PR China

^c College of Optoelectronic Engineering, Shenzhen University, Shenzhen, Guangdong, 518060, PR China

ARTICLE INFO

Keywords:

Molecularly imprinted polymer
ZnIn₂S₄
“On-off” BPE-ECL sensing Platform
Interference-free
Newborn calf serum

ABSTRACT

Herein, a novel molecularly imprinted polymer (MIP) modified spatial-resolved “on-off” ratiometric electrochemiluminescence (ECL) sensing platform based on a closed bipolar electrode (BPE) has been reported for highly accurate and selective detection of ascorbic acid (AA). AA-imprinted MIP was decorated on the anode of the BPE, and Ru (bpy)₃²⁺ in the anode electrolyte served as anode-emitter, while ZnIn₂S₄ as the other ECL emitter was coated on the cathode. Rebinding of AA at anode promoted ECL response of ZnIn₂S₄ (440 nm) at cathode. Meanwhile, the ECL response at 605 nm decreased, arising from the hindered reaction of Ru (bpy)₃²⁺ on the anode surface. Therefore, an “on-off” BPE-ECL sensing platform was fabricated and showed distinguished performance in repeatability and selectivity thanks to the ratio correction effect and the specific recognition from MIP. The linear range for AA detection is from 50 nM to 3 μM with a low detection limit of 20 nM (S/N = 3). The assay deviation of the ratio responses largely declined by about 15 and 5 times compared with the ones from single pole in the aspect of repeatability and long-term stability, respectively. This work provides a reliable and stable sensing pattern for practical application, which also furnishes a strategy for designing simple and low-cost ECL sensing devices.

1. Introduction

Electrochemiluminescence (ECL) based instruments have been widely used as commercial equipment due to its unique features, including simplified optical setup, high sensitivity, easy operation, etc (Miao, 2008). Thereupon, a variety of signal probes have been developed for different applications and showed excellent performance (Chen et al., 2016; Gui et al., 2016; Ma et al., 2015). However, poor robustness of ECL technique presents tremendous barriers for its practical detection. In recent years, the ratiometric concept has been introduced into ECL sensors (Cao et al., 2018a; Zhao et al., 2015). Thanks to the built-in correction, the final ratiometric response between detection and reference signals can substantially make up systematic and random errors derived from power source, environment, personal factors, etc. Up to now, ratiometric ECL sensors have been developed for analyzing a variety of substances like metal ions (Cheng et al., 2014; Lei et al., 2015),

proteins (Feng et al., 2015; Huang et al., 2016), and cancer cells (Wang et al., 2016a). However, a challenge that accompanies ratio-signal sensor is how to avert cross reaction induced by two ECL substances together with their co-reactants in the same reaction cell (Cao et al., 2018b). To settle this problem, several spatial-resolved ECL ratiometric platforms have been proposed by physically separating different ECL emitters. Among them, closed BPE has been constructed for this need, wherein anode and cathode compartments are physically separated. Such design is able to inhibit mutual interference since it possesses dividing emitter settings, and isolated reaction containers as well (Fosdick et al., 2013; Wang et al., 2016b). Furthermore, it extends the choice of applicable materials for functional modification.

It is known that ECL is a highly sensitive approach, and quite susceptible to the influence from environment and sample matrix. To address this issue, functional decoration of ECL sensor is necessary to provide specific recognition toward target analyte. MIP as artificial

* Corresponding author.

** Corresponding author. College of Science, Harbin Institute of Technology, Shenzhen, Guangdong, 518055, PR China.

E-mail addresses: zcpeng@szu.edu.cn (Z. Peng), liyingchun@hit.edu.cn (Y. Li).

<https://doi.org/10.1016/j.bios.2020.112490>

Received 5 June 2020; Received in revised form 16 July 2020; Accepted 31 July 2020

Available online 31 July 2020

0956-5663/© 2020 Elsevier B.V. All rights reserved.

antibody possesses significant advantages, including specific recognition ability, low cost, inherent robustness, etc. Therefore, introduction of MIP is supposed to afford sensor with specificity together with stability and cost-effectiveness (Mayes and Mosbach, 1997). As far as we examined the literatures, a ratio ECL sensor involving molecular imprinting technique (MIT) and BPE strategy has never been reported till now.

Herein, we developed a novel “on-off” BPE-ECL ratiometric platform and fully tested its quantitative performance by taking ascorbic acid (AA) as the model analyte. It is worth to note that this sensing system owns satisfactory detection limit without using any sensitization modification. The construction and composition of the platform is exhibited in Scheme 1. MIP was decorated at the anode for target recognition (Fig. S1) and Ru (bpy)₃²⁺ in the anode reservoir served as ECL anode-emitter, while ZnIn₂S₄ as the ECL cathode-emitter was drop-coated on the surface of the cathode. It is also the first application of ZnIn₂S₄ as ECL emitter to construct ECL sensors. Motivated by the driving electrode, oxidation of Ru (bpy)₃²⁺ at the anode and reduction of ZnIn₂S₄ at the cathode occurred simultaneously, yielding two ECL emission signals with different emission wavelengths. In the presence of AA molecules, the anode response from Ru (bpy)₃²⁺ decreased due to AA binding by MIP, and meanwhile the cathode response increased. Concentration of AA was therefore obtained by calculating the current ratio of the cathode and the anode ($I_{\text{cat}}/I_{\text{ano}}$). The proposed ratio sensor was further applied to determine AA in newborn calf serum.

2. Results and discussion

2.1. Characterization of ZnIn₂S₄

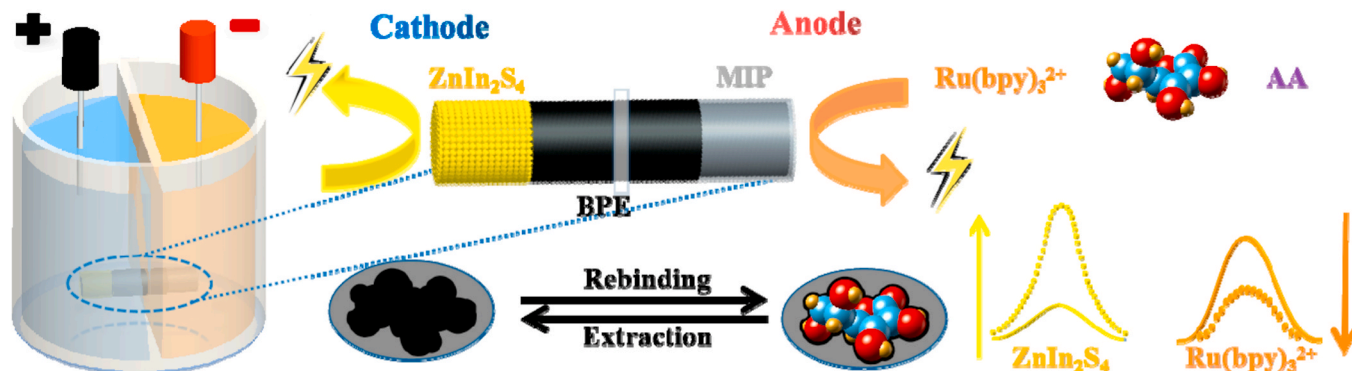
Representative scanning electron microscopy (SEM) images of ZnIn₂S₄ (Fig. 1A) show nanoflower-like morphology with average diameter around 3–4 μm, and its petals present thin nanosheet hierarchy. Energy dispersive spectrometry (EDS) (Fig. 1B) reveals the successful preparation of ZnIn₂S₄ (Salavati-Niasari et al., 2013). X-ray powder diffraction (XRD) spectrum was recorded to identify the crystal structure. As can be seen in Fig. 1C, the typical XRD peaks at 22.4°, 28.4°, 30.4°, 39.9°, 47.2°, 52.4° and 55.8°, respectively correspond to the lattice plane {006}, {102}, {104}, {108}, {110}, {116} and {022} of hexagonal ZnIn₂S₄ (JCPDS-03-065-2023) (Yuan et al., 2014). As shown in Fig. 1D, the X-ray photoelectron spectroscopy (XPS) spectrum of the S 2p region can be divided into two peaks at 161.95 eV and 163.03 eV, which agree well with the S²⁻ valence state (Liu et al., 2014). The characteristic peaks in regional spectrum of Zn 2p (Fig. 1E) and In 3d (Fig. 1F) are consistent with the typical binding energy peaks for Zn²⁺ and In³⁺ (Li et al., 2017). Fig. 1G exhibits the ECL responses of ZnIn₂S₄ in six consecutive potential scanings. Relative standard deviation (RSD) of the emission responses was lower than 5%, confirming excellent repeatability of the obtained ZnIn₂S₄ crystals.

2.2. Fabrication and characterization of BPE

Scheme 1 illustrates construction and composition of the “on-off” ratiometric BPE-ECL sensing platform. ZnIn₂S₄ and MIP were modified respectively at the cathode and the anode of a graphite rod electrode (GRE), which was then placed into the reaction cell (see the details in supporting information, Fig. S2). Electrolyte in the anode compartment is phosphate buffered saline (PBS) with 0.125 mM Ru (bpy)₃²⁺ and 6.25 mM tri-n-propylamine (TPrA), while the cathode compartment is filled with PBS containing 0.1 M K₂S₂O₈. Under the excitation of cyclic voltammetry (CV) scanning in 0–1.2 V, Ru (bpy)₃²⁺ was oxidized at anode, accompanied by simultaneous reduction of ZnIn₂S₄ at cathode. The generated ECL emission signals were located at different emission wavelengths and named as I_{ano} and I_{cat} . Adsorption of AA by MIP layer when the anode was immersed in AA solution prohibits transfer of Ru (bpy)₃²⁺ onto electrode surface, thus causing decrease of I_{ano} (Lach et al., 2019; Sharma et al., 2019; Yang et al., 2019). In addition, AA as electroactive agents can be oxidized at low potential (Cheng et al., 2015), resulting in decreased number of electrons provided for Ru (bpy)₃²⁺ oxidation. In contrast, rebinding of AA at anode promotes the electronic transmission capacity of MIP, thus facilitating the faradic current flowing through the GRE and elevating the I_{cat} value (Malinauskas et al., 2004; Zhang et al., 2018). Therefore, AA adsorption exhibited apparent enhancing effect on I_{cat} and inhibiting effect on I_{ano} , suggesting the feasibility of building ratio-based methodology using the fabricated BPE-ECL platform.

Surface morphology of the BPE anode was characterized by SEM. As observed in Fig. 2A and B, after MIP deposition, the structure of MIP/GRE showed no obvious change and only the thickness of the graphite flakes increased, implying formation of polymeric membrane over the GRE surface. After extraction of AA from MIP/GRE (Fig. 2C), the morphology of polymer membrane scarcely changed, reflecting firmness of MIP film. What is more, we applied differential pulse voltammetry (DPV) to track the synthesis process of MIP and validate removal of template molecules. As shown in Fig. 2D, a wide peak exists after MIP decoration, which might be attributed to oxidation of AA molecules that were embedded in the network of electropolymerized *o*-phenylenediamine. After removal of template molecules, the peak vanishes due to no electroactive substances encapsulated within the MIP layer. Re-exposure of MIP/GRE to AA solution brought about their specific binding and a distinct peak appears as the result of oxidation of the sorbed AA.

The electrochemical behavior of differently modified GRE was monitored by CV in [Fe(CN)₆]^{3-/4-} solution (Fig. 2E). After MIP modification, the redox peak currents of [Fe(CN)₆]^{3-/4-} decreased significantly due to the poor electrical conductivity of poly-*o*-phenylenediamine and the densely-blanketed MIP membrane. Therefore, electrochemical reaction of the embedded AA molecules was inhibited, so was [Fe(CN)₆]^{3-/4-} in electrolyte. Subsequently, the curve of the



Scheme 1. Schematic presentation of the spatially-resolved “on-off” ratiometric BPE-ECL sensing platform for AA monitoring based on a molecularly imprinted polymer modified bipolar electrode.

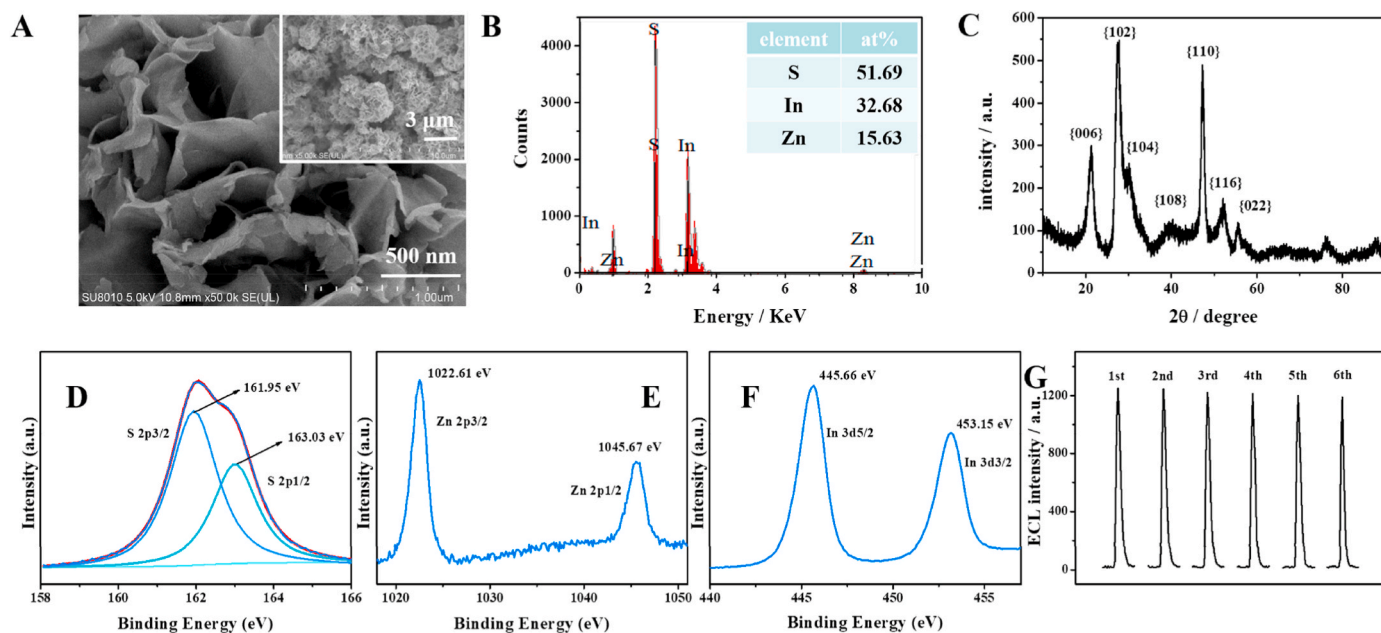


Fig. 1. (A) Representative SEM image of ZnIn_2S_4 . Inset is the corresponding image at lower magnification. (B) EDS spectra of ZnIn_2S_4 . (C) The corresponding XRD pattern of ZnIn_2S_4 . XPS spectra of ZnIn_2S_4 : (D) S 2p, (E) Zn 2p, and (F) In 3d. (G) Repeatability of ECL intensity response of ZnIn_2S_4 under six continuous CV scanning in PBS (pH7.0) containing 0.1 M $\text{K}_2\text{S}_2\text{O}_8$.

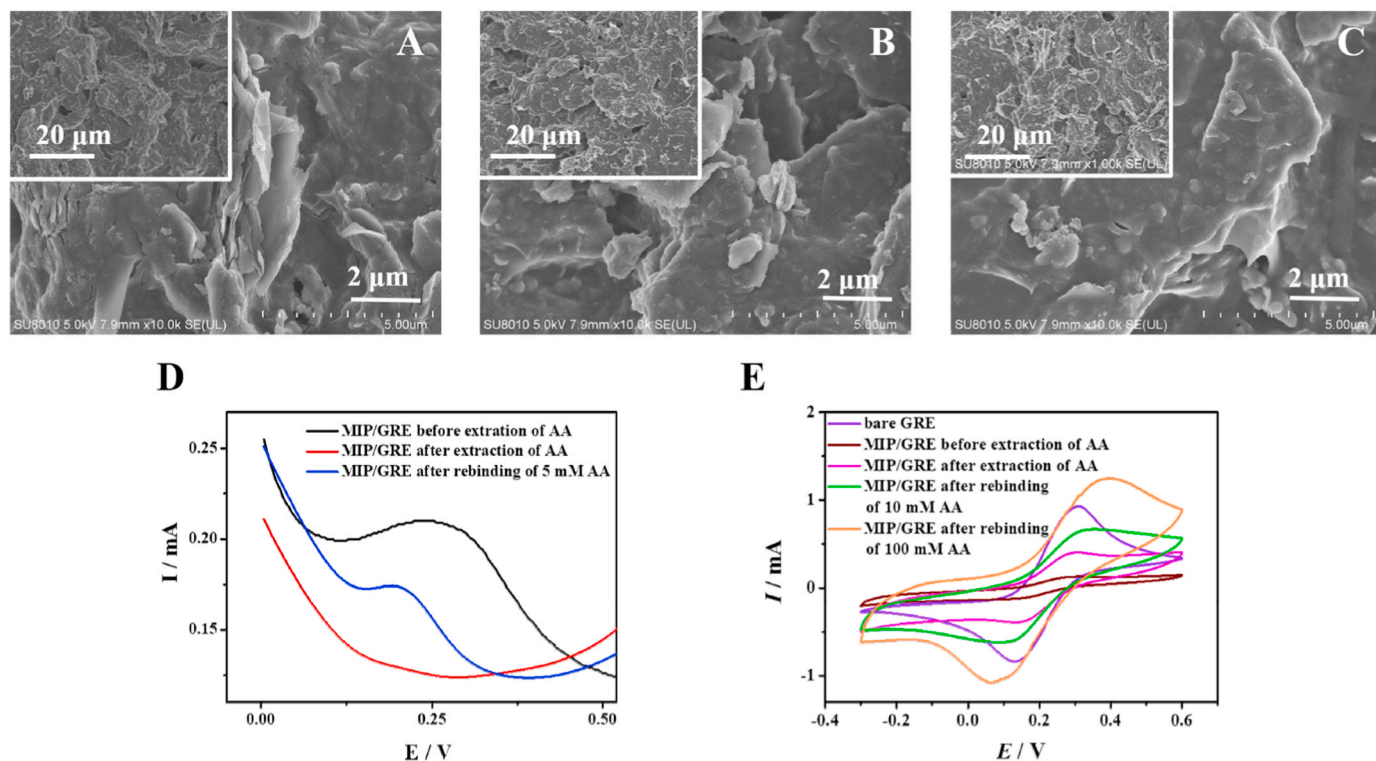


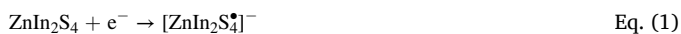
Fig. 2. Representative SEM images of (A) bare GRE, MIP/GRE (B) before and (C) after extraction of AA. Insets are the corresponding images at lower magnification. (D) DPV responses of different GREs in PBS (pH7.0). DPV experiments were performed with amplitude of 50 mV. Pulse width and pulse period was 50 ms and 0.5 s, respectively. (E) CV curves of different GREs in 0.1 M KCl aqueous solution containing 5 mM $[\text{Fe}(\text{CN})_6]^{3-/4-}$. Scan rate was set at 50 mV s^{-1} .

MIP/GRE after extraction of AA displays apparent elevation of redox peaks, owing to formation of the AA-imprinted cavities in the MIP. These cavities served as electron transfer channels for $[\text{Fe}(\text{CN})_6]^{3-/4-}$ ions. After overnight immersion in water, the MIP chains may get loose, and consequently the electrolyte infiltrated into the polymer and generated redox currents. Re-exposure of MIP/GRE to AA led to further increase of

the peak currents, mainly ascribed to contribution from the rebound AA. AA molecules are electroactive and their electrochemical reactions resulted in enhancement of the peak current. This is why MIP/GRE after rebinding higher-concentration AA showed larger peak currents.

2.3. Sensing principle and performance for AA detection

When the BPE sensor underwent CV scanning from 0 to 1.2 V, ZnIn_2S_4 at cathode emitted ECL response centered at 440 nm, while $\text{Ru}(\text{bpy})_3^{2+}$ at anode showed an ECL emission peak at 605 nm (Fig. S3). The ECL mechanism at the anode pole is given in Eqs. S (1)–(3), in which TPrA acts as a co-reactant and participates in excitation of $\text{Ru}(\text{bpy})_3^{2+}$ (Dong et al., 2016; Liu et al., 2015). In the cathode compartment, $\text{S}_2\text{O}_8^{2-}$ in PBS serves as the co-reactant of ZnIn_2S_4 , and the possible mechanism is elucidated in Eqs. (1)–(5). Briefly, ZnIn_2S_4 is electron-injected and turns into negatively charged species ($[\text{ZnIn}_2\text{S}_4]^-$). Meanwhile, $\text{S}_2\text{O}_8^{2-}$ is reduced to oxidant ($[\text{SO}_4]^-$). Thereafter, the radical anion $[\text{ZnIn}_2\text{S}_4]^-$ reacts with $[\text{SO}_4]^-$ and turns to electronically excited state ($\text{ZnIn}_2\text{S}_4^*$). The subsequent relaxation of $\text{ZnIn}_2\text{S}_4^*$ to ground state is accompanied by emission of light.



When CV scanning was applied, oxidation of $\text{Ru}(\text{bpy})_3^{2+}$ occurred in the anode compartment, accompanied by the reduction of ZnIn_2S_4 in the cathode compartment. I_{ano} decreases with the increasing of AA

concentration, while I_{cat} increases (Fig. 3A). As can be found in Fig. 3B and C, I_{cat} and I_{ano} responses were positively and negatively correlated with the logarithm of AA concentration, respectively. As illustrated in Fig. 3D, the ratio of ECL response signals ($I_{\text{cat}}/I_{\text{ano}}$) is proportional to the logarithm of AA concentration, and the linear equation is $I_{\text{cat}}/I_{\text{ano}} = 26.619 + 3.599 \lg C_{\text{AA}} \text{ (nM)}$ ($R^2 = 0.982$). Under the optimal experimental conditions (Fig. S4), it was seen that the fabricated BPE-ECL sensor exhibited a linear relationship in the range of 50–3000 nM, and the detection limit was 20 nM ($S/N = 3$). Table S1 is a comparison among several reported ECL sensors for AA detection. Without modification of extra sensitizing material, our BPE-ECL sensor presents comparable or better performance in the aspects of sensitivity and detection range.

To appraise its feasibility in real-sample detection, the fabricated sensor was applied to determine AA in newborn calf serum. As shown in Table 1, the recovery values measured via standard addition method is in the range of 98.7%–100.8%, indicating good accuracy of the sensor. The same serum samples were detected in parallel using high performance liquid chromatography (HPLC) as a “gold” method, of which the results agree well with the newly developed sensing system, demonstrating decent reliability and validity.

2.4. Assessment of the ratio ECL platform

To compare repeatability of the testing results from the two poles with their ratio values, I_{ano} and I_{cat} were recorded by 15 consecutive tests with 100 nM AA solution. It can be seen in Fig. 4A that both I_{cat} and

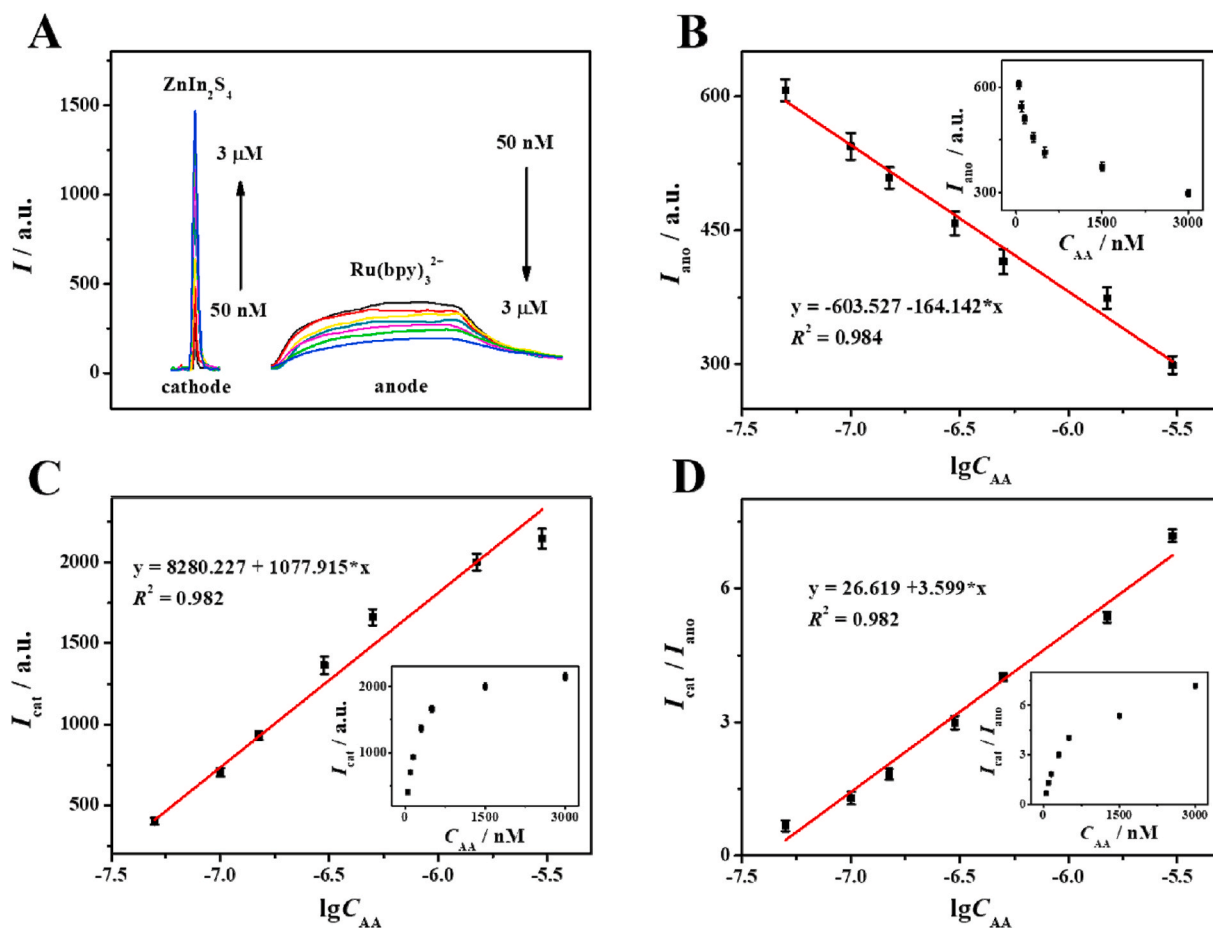


Fig. 3. (A) ECL responses (I) to different concentrations of AA (50 nM–3 μM). The anode reservoir is PBS (pH7.0) containing 0.125 mM $\text{Ru}(\text{bpy})_3^{2+}$ and 6.25 mM TPrA and the cathode reservoir is PBS (pH7.0) containing 0.1 M $\text{K}_2\text{S}_2\text{O}_8$. The calibration curves correlating (B) the anode ECL responses (I_{ano}), (C) the cathode ECL responses (I_{cat}), and (D) ratio responses ($I_{\text{cat}}/I_{\text{ano}}$) with the logarithm of concentration of AA ($\lg C_{\text{AA}}$). Insets are ECL responses correlating concentration of AA (C_{AA}). ECL measurements were motivated by CV scanning from 0 to 1.2 V. Error bars represent the standard deviation from three parallel measurements.

Table 1

Determination results of AA in newborn calf serum using the fabricated sensor and HPLC (n = 3).

Serum samples	Added (μM)	Found by HPLC (μM) ^a	Found by sensor (μM) ^a	Recovery (%)
1	0	1.023 \pm 0.022	1.021 \pm 0.017	–
	10	11.015 \pm 0.027	11.008 \pm 0.020	99.8
	20	21.015 \pm 0.018	21.043 \pm 0.032	100.1
2	0	0.912 \pm 0.008	0.907 \pm 0.022	–
	10	10.883 \pm 0.010	10.781 \pm 0.014	98.7
	20	20.810 \pm 0.016	20.712 \pm 0.018	99.0
3	0	0.945 \pm 0.015	0.932 \pm 0.024	–
	10	10.841 \pm 0.018	10.825 \pm 0.014	98.9
	20	21.034 \pm 0.024	21.088 \pm 0.027	100.8

^a The data are presented as the mean \pm standard deviation.

I_{ano} decreases with the increase of testing times, while the ratio signal ($I_{\text{cat}}/I_{\text{ano}}$) remains almost constant. RSD value of the ratiometric results is 15 times lower than that of single-pole results (n = 15). Long-term stability was also investigated, during which the sensing cell was stored dry at 4 °C and used to measure 500 nM AA sample every day. There is no distinct alteration in $I_{\text{cat}}/I_{\text{ano}}$ response after 25 days despite the decrement of I_{cat} and I_{ano} (Fig. 4B). RSD of the ratiometric platform is 5 times lower compared with the single-pole results (n = 25). These tests fully manifest the distinguished robustness of the ratiometric BPE-ECL sensor.

Selectivity was evaluated by testing sensor responses towards 500 nM urea, uric acid (UA), dopamine (DA), glucose, AA, and their mixture solution. As displayed in Fig. 4C, the sensing responses towards samples containing AA are significantly different from these interferents with a significant level of 0.01. Meanwhile, negligible difference can be observed between the responses from pure AA sample and the mixture with a significant level of 0.05. The good selectivity is very likely to do

with the specific recognition contributed by MIP membrane. In a word, thanks to the superior selectivity of MIP and the preeminent robustness of ratiometric BPE-ECL sensor, the “on-off” ratiometric platform can be employed for accurate and selective determinate of AA.

3. Conclusion

We reported a novel MIP modified “on-off” ratiometric electrochemiluminescence (ECL) sensing pattern based on a closed bipolar electrode (BPE). It is the first ratio ECL sensor involving molecular imprinting technique and BPE strategy, in which ZnIn_2S_4 as the cathode-emitter was employed in constructing ECL sensor for the first time. Cross reaction can be effectively avoided due to the inherent characteristic of BPE that the different reactions take place at spatial-resolved poles. The ECL signals from the two electrode poles with “on-off” response mode constituted a ratio value for quantitative analysis, exhibiting excellent robustness and reliability. The fabricated platform showed great sensing performance toward the model analyte-AA, displaying relatively wide linear range, low detection limit, excellent selectivity and repeatability. Taking the innate advantage of high sensitivity of ECL technology, it is worth to note that this sensing system generated satisfactory detection limit without any extra sensitization modification. With all these merits, the “on-off” ratiometric BPE-ECL sensor is expected to provide a universal methodology for designing ECL sensors with high robustness and selectivity.

CRediT authorship contribution statement

Yue Hu: Methodology, Software, Data curation, Writing - original draft. **Yongcheng He:** Writing - review & editing. **Zhengchun Peng:** Writing - review & editing. **Yingchun Li:** Writing - review & editing, Supervision.

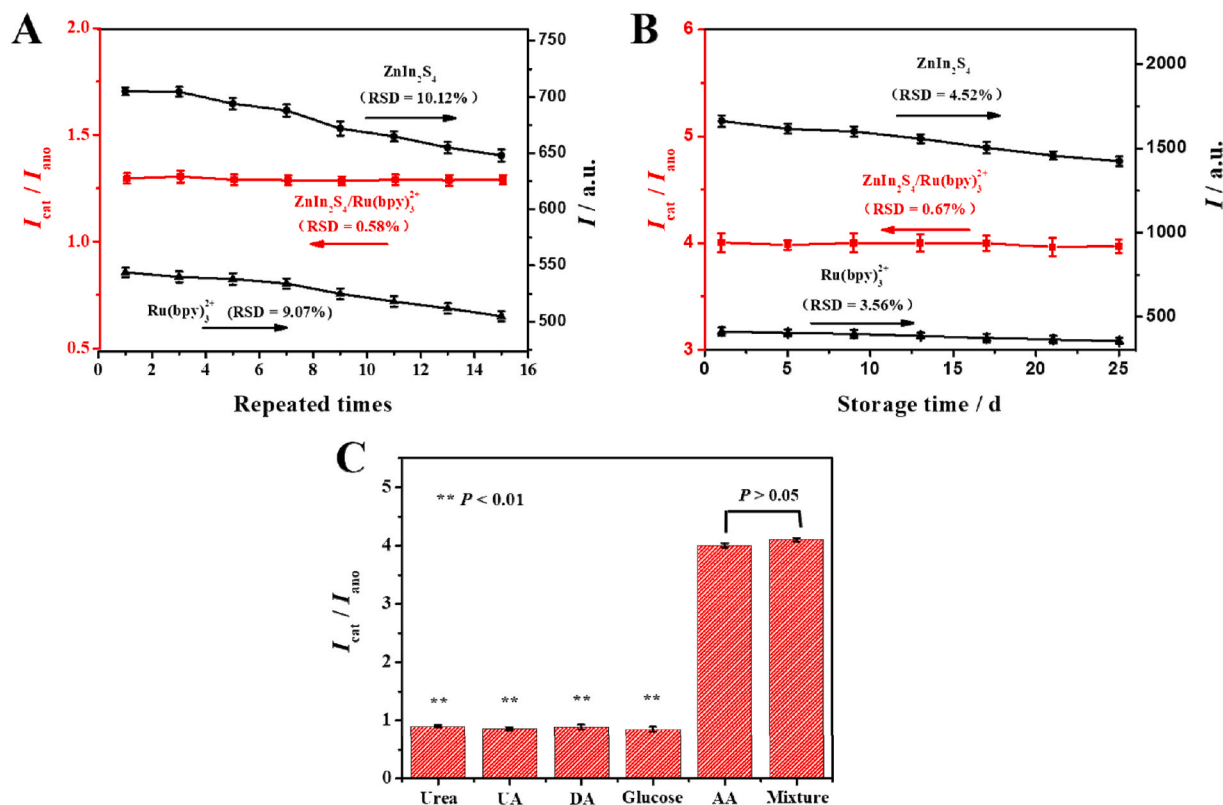


Fig. 4. Plots of ECL responses versus (A) repeated times and (B) storage time. (C) ECL responses of the BPE-ECL sensor after successive incubation in 500 nM urea, UA, DA, glucose, AA, and their mixture solution. ECL measurements were motivated by CV scanning from 0 to 1.2 V. Error bars represent the standard deviation from three parallel measurements.

Declaration of competing interest

The authors declare that they have no known competing financial interests or personal relationships that could have appeared to influence the work reported in this paper.

Acknowledgments

The work financially supported by Shenzhen Science and Technology Program (Grant No. KQTD20170810105439418, KQJSCX20180328165437711) and National Natural Science Foundation of China (81973280, 81773680).

Appendix A. Supplementary data

Supplementary data related to this article can be found at <https://doi.org/10.1016/j.bios.2020.112490>.

References

- Cao, J.-T., Wang, Y.-L., Wang, J.-B., Zhou, Q.-M., Ma, S.-H., Liu, Y.-M., 2018a. *J. Electroanal. Chem.* 814, 111–117.
- Cao, J.-T., Wang, Y.-L., Zhang, J.-J., Dong, Y.-X., Liu, F.-R., Ren, S.-W., Liu, Y.-M., 2018. *Anal. Chem.* 90 (17), 10334–10339.
- Chen, A., Ma, S., Zhuo, Y., Chai, Y., Yuan, R., 2016. *Anal. Chem.* 88 (6), 3203–3210.
- Cheng, H., Wang, X., Wei, H., 2015. *Anal. Chem.* 87 (17), 8889–8895.
- Cheng, Y., Huang, Y., Lei, J., Zhang, L., Ju, H., 2014. *Anal. Chem.* 86 (10), 5158–5163.
- Dong, Y.-P., Zhou, Y., Wang, J., Zhu, J.-J., 2016. *Anal. Chem.* 88 (10), 5469–5475.
- Feng, X., Gan, N., Zhang, H., Yan, Q., Li, T., Cao, Y., Hu, F., Yu, H., Jiang, Q.J.E.A., 2015. *Electrochim. Acta* 170, 292–299.
- Fosdick, S.E., Knust, K.N., Scida, K., Crooks, R.M., 2013. *Bipolar electrochemistry*. *Angew. Chem. Int. Ed.* 52 (40), 10438–10456.
- Gui, G.-F., Zhuo, Y., Chai, Y.-Q., Xiang, Y., Yuan, R., 2016. *Biosens. Bioelectron.* 77, 7–12.
- Huang, Y., Lei, J., Cheng, Y., Ju, H., 2016. *Biosens. Bioelectron.* 77, 733–739.
- Lach, P., Cieplak, M., Majewska, M., Noworyta, K.R., Sharma, P.S., Kutner, W., 2019. *Anal. Chem.* 91 (12), 7546–7553.
- Lei, Y.-M., Huang, W.-X., Zhao, M., Chai, Y.-Q., Yuan, R., Zhuo, Y., 2015. *Anal. Chem.* 87 (15), 7787–7794.
- Li, W., Lin, Z., Yang, G., 2017. *Nanoscale* 9 (46), 18290–18298.
- Liu, Q., Lu, H., Shi, Z., Wu, F., Guo, J., Deng, K., Li, L., 2014. *ACS Appl. Mater. Interfaces* 6 (19), 17200–17207.
- Liu, R., Zhang, C., Liu, M., 2015. *Sensor. Actuator. B Chem.* 216, 255–262.
- Ma, M.-N., Zhuo, Y., Yuan, R., Chai, Y.-Q., 2015. *Anal. Chem.* 87 (22), 11389–11397.
- Malinauskas, A., Garjonytė, R., Mazeikienė, R., Jurevičiūtė, I., 2004. *Talanta* 64 (1), 121–129.
- Mayes, A.G., Mosbach, K., 1997. *Trac. Trends Anal. Chem.* 16 (6), 321–332.
- Miao, W., 2008. *Chem. Rev.* 108 (7), 2506–2553.
- Salavati-Niasari, M., Ranjbar, M., Sabet, M., 2013. *Journal of Inorganic Organometallic Polymers Materials Science and Engineering: Chimia* 23 (2), 452–457.
- Sharma, P.S., Garcia-Cruz, A., Cieplak, M., Noworyta, K.R., Kutner, W., 2019. *Current Opinion in Electrochemistry* 16, 50–56.
- Wang, Y.-Z., Hao, N., Feng, Q.-M., Shi, H.-W., Xu, J.-J., Chen, H.-Y., 2016. *Biosens. Bioelectron.* 77, 76–82.
- Wang, Y.-Z., Zhao, W., Dai, P.-P., Lu, H.-J., Xu, J.-J., Pan, J., Chen, H.-Y., 2016b. *Biosens. Bioelectron.* 86, 683–689.
- Yang, J., Hu, Y., Li, Y., 2019. *Biosens. Bioelectron.* 135, 224–230.
- Yuan, L., Yang, M.-Q., Xu, Y., 2014. *J. Mater. Chem.* 2 (35), 14401–14412.
- Zhang, L., Wang, G., Wu, D., Xiong, C., Zheng, L., Ding, Y., Lu, H., Zhang, G., Qiu, L.J.B., 2018. *Biosens. Bioelectron.* 100, 235–241.
- Zhao, H.-F., Liang, R.-P., Wang, J.-W., Qiu, J.-D., 2015. *Chem. Commun.* 51 (63), 12669–12672.